JOURNAL OF BACTERIOLOGY, Oct. 2003, p. 6209–6214 Vol. 185, No. 20
0021-9193/03/$08.00+0 DOI: 10.1128/JB.185.20.6209–6214.2003

Characterization of *divIVA* and Other Genes Located in the Chromosomal Region Downstream of the *dcw* Cluster in *Streptococcus pneumoniae*†

Daniela Fadda,[1] Carla Pischedda,[1] Fabrizio Caldara,[2] Michael B. Whalen,[1] Daniela Anderluzzi,[2] Enrico Domenici,[2] and Orietta Massidda[1]*

Dipartimento di Scienze Chirurgiche Sez. Microbiologia, Università di Cagliari, 09100 Cagliari,[1] and GlaxoSmithKline Medicines Research Center, 37100 Verona,[2] Italy

Received 16 June 2003/Accepted 14 July 2003

We analyzed the chromosome region of *Streptococcus pneumoniae* located downstream of the division and cell wall (*dcw*) cluster that contains the homolog of the *Bacillus subtilis* cell division gene *divIVA* and some genes of unknown function. Inactivation of *divIVA* in *S. pneumoniae* resulted in severe growth inhibition and defects in cell shape, nucleoid segregation, and cell division. Inactivation of the *ylm* genes resulted in some morphological and/or division abnormalities, depending on the inactivated gene. Transcriptional analysis revealed a relationship between these genes and the *ftsA* and *ftsZ* cell division genes, also indicating that the connection between the *dcw* cluster and the *divIVA* region is more extensive than just chromosomal position and gene organization.

Historically, most of the available information about bacterial cell division comes from the intensively studied gram-negative rod *Escherichia coli* and the gram-positive rod *Bacillus subtilis* (reviewed in references 1, 9, 10, 15, 17, and 24). This situation is changing, due to both the increasing interest in the field of cell division and the availability of genomic data. Most of the cell division genes have now been identified in a wide range of bacteria, and despite the differences observed among species, many of these genes are found organized in a chromosomal region corresponding to the 2-min region of the *E. coli* chromosome known as the *dcw* (for "division and cell wall") cluster.

Notwithstanding the large amount of sequence information, very little is known about the molecular mechanism that regulates cell division in bacteria other than the model organisms and cell division in gram-positive cocci remains poorly understood. However, some extrapolations from the analysis of the Fts proteins that are essential for cell division, in particular the FtsZ protein, the major component of the septal ring structure (15), suggest that the basic mechanism involved in septum formation should not differ from cocci to rods.

A more intriguing problem and one that shows significantly less conservation is how different bacteria operate the division site selection mechanism that ensures correct FtsZ positioning at midcell. In *E. coli*, the correct division site at the center is distinguished from the other potential division sites at the poles through the combined action of three proteins, MinC, MinD, and MinE, encoded by the *minCDE* genes (5, 6, 21).

In *B. subtilis*, *divIVB* encodes the MinC and MinD homologs but not the MinE homolog (13, 26). The DivIVA protein has been proposed to play a role in the control of division site selection as the functional counterpart of the missing MinE in *B. subtilis* (3, 7, 18, 19).

Recently, we identified a *Streptococcus pneumoniae* gene encoding the *B. subtilis* DivIVA homolog (20). We noted that *divIVA* is the last gene of a region located downstream of the cell division genes *ftsA* to *ftsZ* and is conserved in the same position in a number of gram-positive cocci. In addition to *divIVA*, the region contains some open reading frames of unknown function, designated *ylmD*, *ylmE*, *ylmF*, *ylmG*, and *ylmH*, all transcribed in the same direction as the *dcw* genes. In streptococci the first gene of the cluster, *ylmD*, is missing (20).

Both chromosomal position and gene organization suggested that these genes may be involved in cell division, sparking our interest in their characterization.

The function of *divIVA* and the *ylm* genes in *S. pneumoniae* was analyzed by insertion-deletion mutagenesis. Constructs for gene inactivation were obtained by a two-step PCR method. Three sets of primers (sequences available on request) were used for each construct. PCR products were amplified from the appropriate template DNA by using 1 U of *Taq* polymerase (Perkin-Elmer) in a Hybaid thermocycler. The first set of primers was used to amplify fragment 1, corresponding to the 5′ end of the gene to be inactivated; the second set was used to amplify the *cat* cassette from pR326 (4); and the third set was used to amplify fragment 2, corresponding to the 3′ end of the gene to be inactivated. PCR-derived fragments were purified by using a PCR purification kit (Qiagen), mixed in the molar ratio of 1:1:1, and reamplified in a second run with the external primers.

Linear constructs containing the *cat* cassette in the middle were obtained for the inactivation of *ylmE*, *ylmF*, *ylmG*, *ylmH*, and *divIVA* and used to transform *S. pneumoniae* wild-type Rx1 strain (20) as previously reported (23). Transformants selected on tryptic soy agar plates supplemented with 5% (vol/vol)

* Corresponding author. Mailing address: Dipartimento di Scienze Chirurgiche Sez. Microbiologia, Via Porcell, 4 Universita di Cagliari, 09100 Cagliari, Italy. Phone: 39-070-6758485. Fax: 39-070-6758485. E-mail: omassid@vaxca1.unica.it.

† This work is dedicated to the memory of Gerald D. Shockman, whose expertise and enthusiasm are greatly missed.

TABLE 1. Relevant features of the null mutant phenotypes

Strain	Doubling time (min)	Phase-contrast morphology	Nucleoid fluorescence[a]	Shape	Cell diameter (μm)[b]	Septum	Transformability[c]
Rx1	32	Diplococci	Parental strain	Normal	0.54 ± 0.022	Symmetrical and well defined	+
Rx1 *ylmE*::*cat*	36	Diplococci	Significantly reduced	Normal	0.60 ± 0.020	Thinner	+
Rx1 *ylmF*::*cat*	36	Chains	As parental	Altered	0.64 ± 0.017	Thinner and incomplete	−
Rx1 *ylmG*::*cat*	42	Diplococci and tetrads	As parental	Normal	0.55 ± 0.013	Thinner	+
Rx1 *ylmH*::*cat*	32	Diplococci and chains	As parental	Normal	0.56 ± 0.014	Thinner	+
Rx1 *divIVA*::*cat*	56	Chains	Absent in some cells	Altered	0.62 ± 0.022	Incomplete and occasionally oblique	+

[a] DAPI stain flourescence was used to determine the presence and location of the nucleoid.
[b] Cell diameters are given as the means ± the standard deviations calculated by measuring *S. pneumoniae* cells at the same stage of division.
[c] +, colonies were recovered on plates after transformation with plasmid or linear DNA; −, no colonies were recovered on plates after transformation with plasmid or linear DNA.

defibrinated sheep blood containing chloramphenicol (4 μg/ml) were obtained in all cases, indicating that none of these genes is essential to *S. pneumoniae*.

For each disruption, at least four transformants showing the correct insertion, as verified by PCR, were further analyzed. The different phenotypic characteristics of the *divIVA*::*cat* and each of the *ylm*::*cat* mutants relative to those of the wild-type Rx1 strain are discussed below and summarized in Table 1.

The *divIVA*::*cat* mutants, although viable, revealed the most dramatic defects with respect to growth, morphology, division, and nucleoid distribution. When cultivated in tryptic soy broth (TSB) medium, *divIVA*::*cat* mutants grew significantly slower then the wild type (Table 1). Phase-contrast microscopy and 4′,6′-diamidino-2-phenylindole (DAPI) staining showed that *divIVA*::*cat* mutants grew as chains of unseparated cells often devoid of nucleoid (Fig. 1). Electron microscopy confirmed the presence of chains with individual cells that lost the lancet-like shape characteristic of pneumococci and showed altered cell diameter, irregular margins, and unclosed division septa at midcell (Fig. 2).

Although the *divIVA* null phenotype may indicate a requirement of *divIVA* for proper septum formation and assembly in *S. pneumoniae*, as suggested by the presence of incomplete septa in cells lacking functional DivIVA, the possibility that both these defects and the presence of anucleate cells may originate from a defect in chromosomal segregation cannot be completely excluded. Additionally, the *divIVA* null phenotype in *S. pneumoniae* differs substantially from the *divIVA* null phenotype in *B. subtilis* (3, 7) and the previously proposed functional homology of DivIVA with MinE does not seem to apply to *S. pneumoniae*.

Recently, Thomaides et al. (25) have shown a second distinct function in chromosomal segregation for the *B. subtilis* DivIVA protein during sporulation. This second function of *B. subtilis* DivIVA better agrees with some features shown by *S. pneumoniae divIVA* null mutants, raising the possibility that the primary role of DivIVA is in chromosomal segregation. Consistent with this possibility is the presence of *divIVA* in bacteria, including gram-positive cocci, that seem to lack en bloc the equivalent of the *min* genes.

Previous protein sequence similarity searches showed that DivIVA has homologs among the gram-positive bacteria (8, 20) and possibly among some eukaryotic coil-coiled proteins (8) but not among gram-negative bacteria. Interestingly, when the DivIVA homologs from high-G+C-content gram-positive bacteria were used as a query sequence in BLAST searches, a significant degree of similarity (data not shown) with the *E. coli* TolA (12) was detected. In support of this observed similarity is the recently reported role of TolA in *E. coli*, in which mutations or deletions in domains II or III of the protein were shown to cause cell division defects (22) very similar to those of the *divIVA* null mutant phenotype reported here for *S. pneumoniae*. However, further studies to identify partner proteins that interact with DivIVA, suppressors of the *divIVA* null phenotype, and cellular localization of DivIVA in *S. pneumoniae* should help to verify the relationship between TolA and DivIVA and to clarify the precise role of DivIVA in cocci.

Inactivation of the *ylm* genes resulted in some morphological and/or division abnormalities, depending on the inactivated gene. Growth in TSB medium showed that all *ylm* mutants had doubling times similar to that of the wild type, with the exception of *ylmG*::*cat* mutants (Table 1). However, phase-contrast microscopy, DAPI staining of the nucleoids, and electron microscopy showed a distinct phenotype for each *ylm* inactivation.

S. pneumoniae ylmE::*cat* mutant cells were similar in shape to but, on average, slightly larger than wild-type cells. However, the fluorescence of their nucleoids appeared greatly reduced (Fig. 1). Electron microscopy of *ylmE*::*cat* cells confirmed the larger size of this mutant and the presence of internal zones that appeared to be less electron dense (Fig. 2).

S. pneumoniae ylmF::*cat* mutants analyzed by phase-contrast microscopy were morphologically different, showing the presence of some sausage-like cells and occasionally of elongated cells and minicells. DAPI staining revealed normal fluorescence in all cells, including minicells, where a guillotine effect

FIG. 1. Phase-contrast analysis of the Rx1 wild-type strain and the insertion-deletion mutants. Bacterial cells were cultured in TSB medium, sampled at selected times during the exponential phase of growth, fixed with 1% (vol/vol) formaldehyde for 15 min at room temperature, treated with DAPI as previously described (2), and examined by using an Axioskop HBO50 equipped with a Plan-Neofluar 100× oil lens. For each strain, phase-contrast (left panels) and DAPI stain fluorescence (right panels) micrographs are shown. The scale bars correspond to 3 μm.

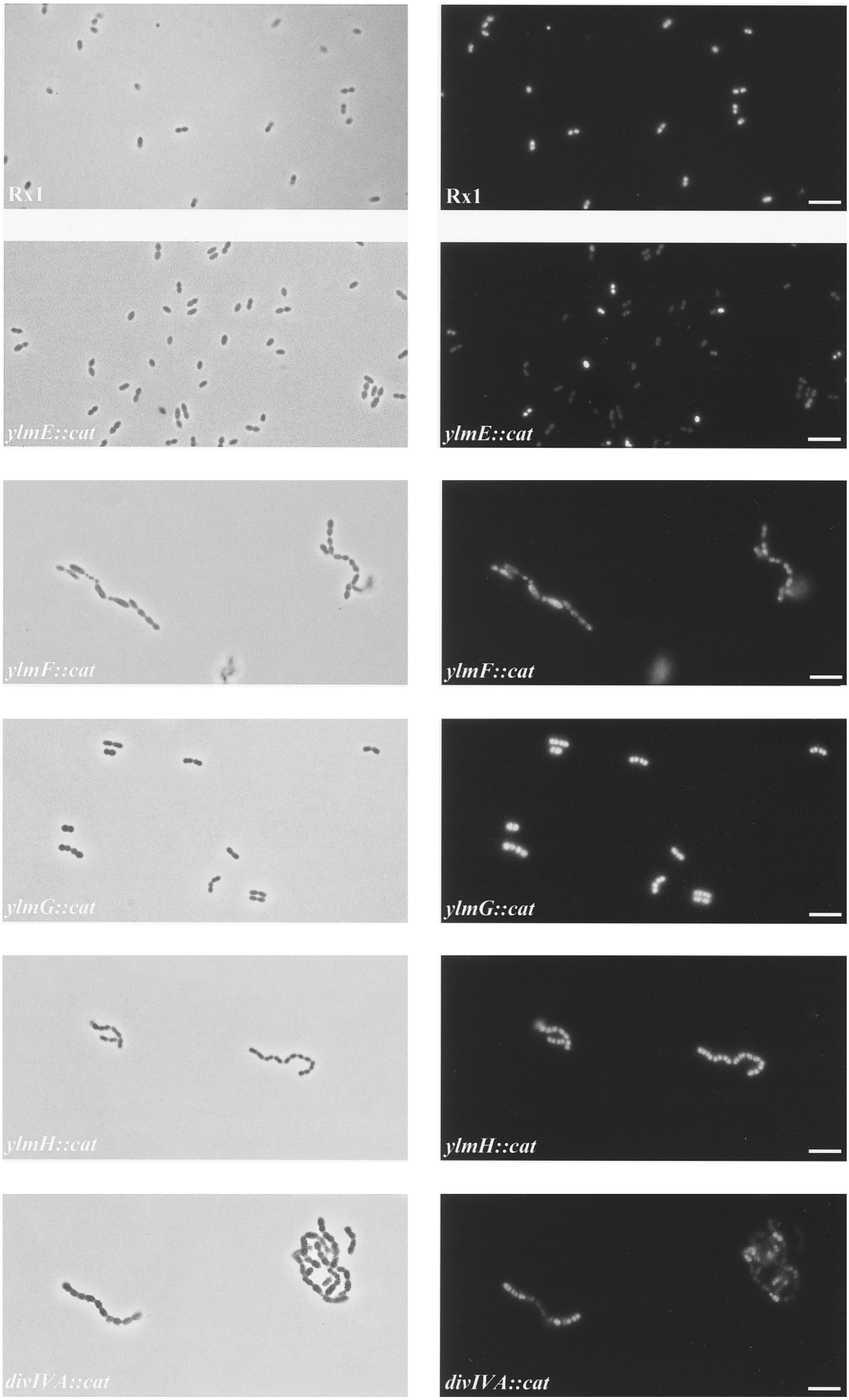

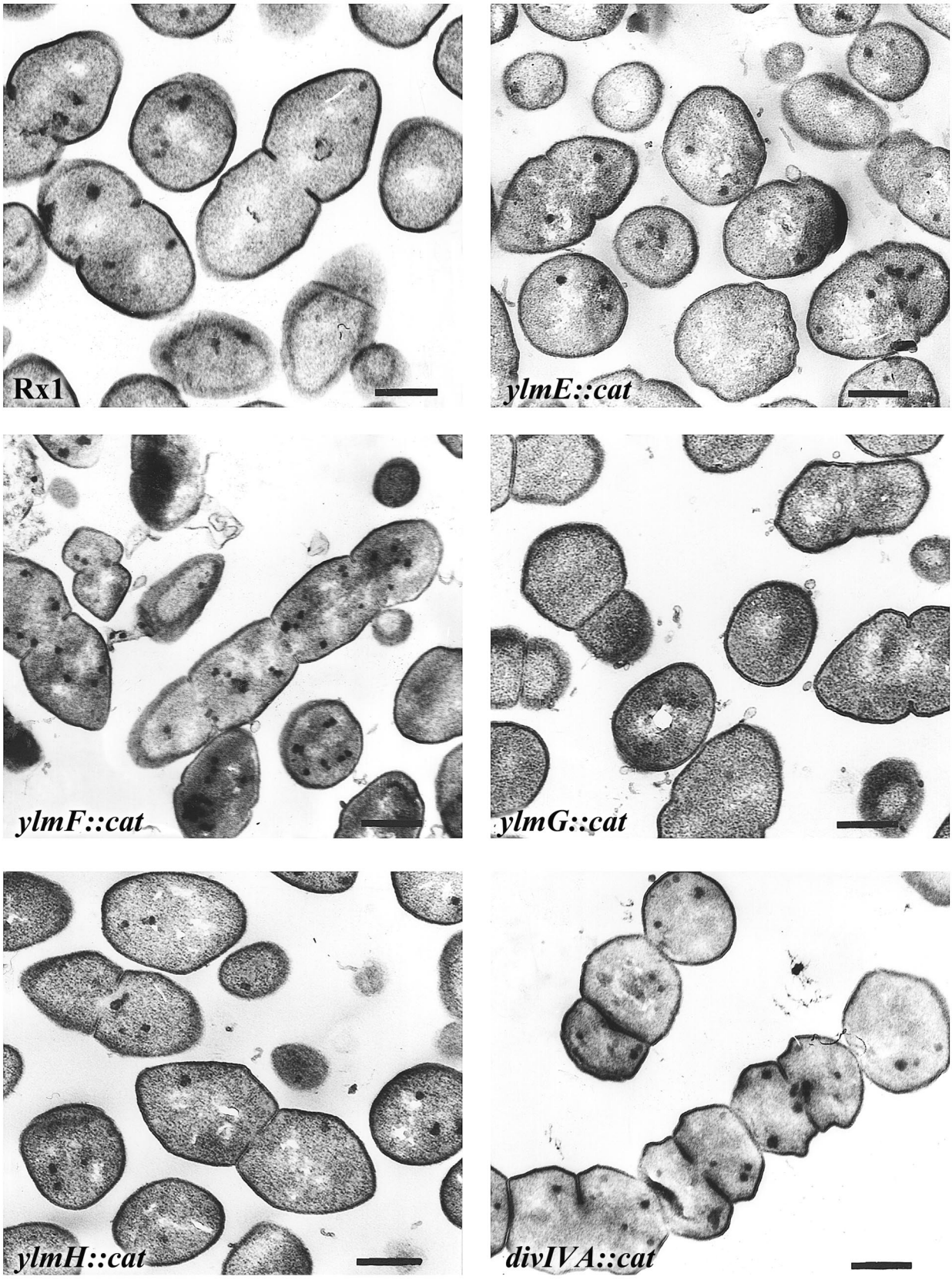

FIG. 2. Electronic transmission analysis of the Rx1 wild-type strain and of the insertion-deletion mutants. Cells were cultured in TSB medium to mid-exponential phase, fixed in 1% (vol/vol) glutaraldehyde for 2 h at room temperature, processed as previously described (11), and then observed and photographed in a Zeiss EM 10 electron microscope. The abnormalities of various null mutants are described in the text and summarized in Table 1. The scale bars correspond to 0.3 μm.

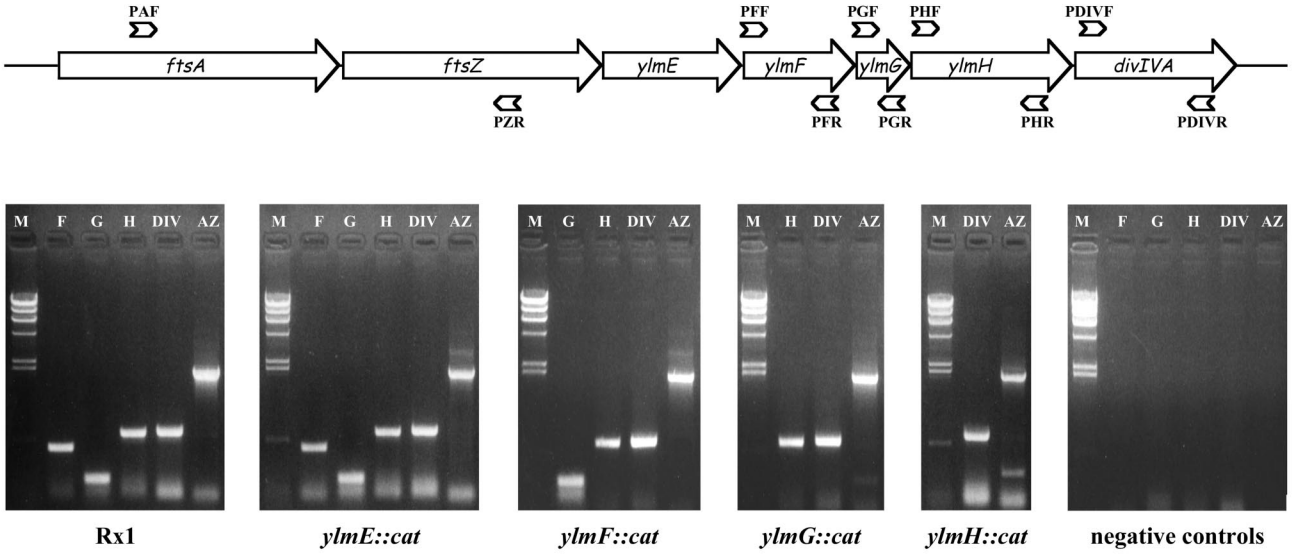

FIG. 3. Transcriptional analysis of the region downstream of each insertion by RT-PCR. The random primer Pd(N)6 or the specific primer PDIVR was used to generate cDNA. Total RNA from the *S. pneumoniae* Rx1 strain and *ylm*::*cat* mutants was used as the template in a reverse transcriptase reaction with primers (PAF, PZR, PFF, PFR, PGF, PGR, PHF, PHR, and PDIVF) internal to each gene. Expression of the genes in the wild-type Rx1 strain and in the insertion-deletion mutants would give products of the following sizes: *ylmF* (F), 477 bp; *ylmG* (G), 202 bp; *ylmH* (H), 661 bp; and *divIVA* (DIV), 663 bp. A positive control, *ftsA-ftsZ* (AZ), 1,902 bp, was included in all reactions. Negative controls included identical reactions to which no cDNA template was added. DNA contamination of the RNA samples was ruled out by performing PCR directly on the RNAs (data not shown). The source of the respective RNA template used for each set of reactions is indicated under each panel. M, *Hin*dIII-digested λ phage.

on the nucleoid was observed (Fig. 1). In the electron micrograph of *ylmF*::*cat* mutants, the multiseptate sausage-like elements with multiple and thinner septa at an early stage of constriction were evident (Fig. 2).

S. pneumoniae ylmG::*cat* mutants did not show any substantial difference in morphology or fluorescence. However, packs of cells resembling tetrads were seen in addition to diplococci in phase-contrast and fluorescence micrographs (Fig. 1). Thinner septa were observed in the electron micrographs (Fig. 2)

S. pneumoniae ylmH::*cat* mutants grew as diplococci or short chains of cells showing the typical pneumococcal shape and normal fluorescence (Fig. 1). However, *ylmH* null cells started lysing before the end of the exponential phase, earlier than the physiological lysis of the wild type. Electron microscopy revealed the presence of diplococci where the most appreciable difference was the presence of thinner septa (Fig. 2).

In addition to the single inactivations, double knockouts were constructed for each individual *ylm*::*cat* mutant. A *divIVA* fragment containing an *erm* cassette from plasmid pVA838 (16) was used to transform each *ylm*::*cat* mutant. Double null mutants were selected on tryptic soy agar blood plates containing chloramphenicol (4 μg/ml) and erythromycin (0.2 μg/ml) for all recipient single null mutants with the exception of the *ylmF*::*cat* strain (Table 1).

All the double mutants obtained (*ylmE*::*cat-divIVA*::*erm*, *ylmG*::*cat-divIVA*::*erm*, and *ylmH*::*cat-divIVA*::*erm*) showed a *divIVA* null phenotype, indicating the epistatic effect of *divIVA* with respect to the other genes and supporting the possibility that the single gene inactivations lack a polar effect on the downstream region.

In the absence of obvious cell division mutants in *S. pneumoniae* and in other gram-positive cocci, the *ylm* null phenotypes were less evident than the *divIVA* null phenotype and the results were more difficult to interpret. However, as suggested by the *ylmF*::*cat* phenotype, *ylmF* may be involved in determining the frequency and position of the septum, a possibility in support of the observation that other, still unknown factors are involved in this process (14). Moreover, although the phenotype of the single *ylmE* and *ylmG* null mutants did not give us any conclusive evidence, the disruption of the pairs *ylmE*::*erm* and *ylmG*::*cat* showed that double mutants divide in multiple planes, in contrast to the single plane used by streptococci (not shown).

The tight organization of the genes located downstream of the *dcw* cluster suggested that in *S. pneumoniae* these genes are transcribed together and possibly also with the adjacent cell division genes *ftsA* and *ftsZ*.

To investigate this possibility, *S. pneumoniae* cells were grown in TSB medium to the mid-exponential phase and total RNA was extracted and used in reverse transcription (RT)-PCR with the cMaster RT_{plus}PCR system. RT-PCR products of the expected sizes were amplified in all cases (data not shown), indicating a transcriptional relationship between these genes. Therefore, to determine if the insertional mutation in the upstream gene would abolish the transcription of the downstream genes by a polar effect, we analyzed the expression of *ylmF*, *ylmG*, *ylmH*, and *divIVA* genes in the wild-type Rx1 strain and in each of the insertion-deletion mutants by RT-PCR. As shown in Fig. 3, we found that, without exception, all the downstream genes were still expressed in each of the mutants, indicating that downstream transcription was not abolished by the *cat* cassette insertion.

Taken together, our results indicate that the relationship between the *dcw* cluster and the *divIVA* region is more extensive than just chromosomal position and gene organization and suggest a complex pattern of transcriptional regulation between the last genes of the *dcw* cluster and the genes located immediately downstream.

This work represents an initial step in elucidating cell division in gram-positive cocci. In particular, it underlines the fact that the molecular mechanisms at the base of this process cannot be extrapolated solely from the information available from other bacteria, including *B. subtilis*. Thus, *S. pneumoniae* can provide a useful model among the gram-positive cocci, due to both the ease of genetic manipulation and the simple mode of division.

This work was supported by Cell Factory Contract no. CT96-0122 from the European Commission (DGXII) Biotechnology Program and by 60% MURST funds to O. Massidda.

We gratefully acknowledge C. Zancanaro and F. Merigo of the Dipartimento di Scienze Morfologico-Biomediche, Università di Verona, and A. Riva of the Servizio di Microscopia Elettronica, Dipartimento di Citomorfologia, Università di Cagliari, for their support in electron microscopy. We thank P. E. Varaldo for critical review of the manuscript.

REFERENCES

1. **Bramhill, D.** 1997. Bacterial cell division. Annu. Rev. Cell Dev. Biol. **13:** 395–424.
2. **Bylund, J. E., M. A. Haines, P. J. Piggot, and M. L. Higgins.** 1993. Axial filament formation in *Bacillus subtilis*: induction of nucleoids of increasing length after addition of chloramphenicol to exponential-phase cultures approaching stationary phase. J. Bacteriol. **175:**886–890.
3. **Cha, J. H., and G. C. Stewart.** 1997. The *divIVA* minicell locus of *Bacillus subtilis*. J. Bacteriol. **179:**1671–1683.
4. **Claverys, J. P., A. Dintilhac, E. V. Pestova, B. Martin, and D. A. Morrison.** 1995. Construction and evaluation of new drug-resistance cassettes for gene disruption mutagenesis in *Streptococcus pneumoniae*, using an *ami* test platform. Gene **164:**123–128.
5. **de Boer, P. A., R. E. Crossley, and L. I. Rothfield.** 1988. Isolation and properties of *minB*, a complex genetic locus involved in correct placement of the division site in *Escherichia coli*. J. Bacteriol. **170:**2106–2112.
6. **de Boer, P. A., R. E. Crossley, and L. I. Rothfield.** 1989. A division inhibitor and a topological specificity factor coded for by the minicell locus determine proper placement of the division septum in *E. coli.* Cell **56:**641–649.
7. **Edwards, D. H., and J. Errington.** 1997. The *Bacillus subtilis* DivIVA protein targets to the division septum and controls the site specificity of cell division. Mol. Microbiol. **24:**905–915.
8. **Edwards, D. H., H. B. Thomaides, and J. Errington.** 2000. Promiscuous targeting of *Bacillus subtilis* cell division protein DivIVA to division sites in *Escherichia coli* and fission yeast. EMBO J. **19:**2719–2727, 5039.
9. **Errington, J., R. A. Daniel, and D. J. Scheffers.** 2003. Cytokinesis in bacteria. Microbiol. Mol. Biol. Rev. **67:**52–65.
10. **Harry, E. J.** 2001. Bacterial cell division: regulating Z-ring formation. Mol. Microbiol. **40:**795–803.
11. **Higgins, M. L., and G. D. Shockman.** 1970. Model for cell wall growth of *Streptococcus faecalis*. J. Bacteriol. **101:**643–648.
12. **Levengood, S. K., and R. E. Webster.** 1989. Nucleotide sequences of the *tolA* and *tolB* genes and localization of their products, components of a multistep translocation system in *Escherichia coli*. J. Bacteriol. **171:**6600–6609.
13. **Levin, P. A., P. S. Margolis, P. Setlow, R. Losick, and D. Sun.** 1992. Identification of *Bacillus subtilis* genes for septum placement and shape determination. J. Bacteriol. **174:**6717–6728.
14. **Levin, P. A., J. J. Shim, and A. D. Grossman.** 1998. Effect of *minCD* on FtsZ ring position and polar septation in *Bacillus subtilis*. J. Bacteriol. **180:**6048–6051.
15. **Lutkenhaus, J., and S. G. Addinall.** 1997. Bacterial cell division and the Z ring. Annu. Rev. Biochem. **66:**93–116.
16. **Macrina, F. L., J. A. Tobian, K. R. Jones, R. P. Evans, and D. B. Clewell.** 1982. A cloning vector able to replicate in *Escherichia coli* and *Streptococcus sanguis*. Gene **19:**345–353.
17. **Margolin, W.** 2000. Themes and variations in prokaryotic cell division. FEMS Microbiol. Rev. **24:**531–548.
18. **Marston, A. L., H. B. Thomaides, D. H. Edwards, M. E. Sharpe, and J. Errington.** 1998. Polar localization of the MinD protein of *Bacillus subtilis* and its role in selection of the mid-cell division site. Genes Dev. **12:**3419–3430.
19. **Marston, A. L., and J. Errington.** 1999. Selection of the midcell division site in *Bacillus subtilis* through MinD-dependent polar localization and activation of MinC. Mol. Microbiol. **33:**84–96.
20. **Massidda, O., D. Anderluzzi, L. Friedli, and G. Feger.** 1998. Unconventional organization of the division and cell wall gene cluster of *Streptococcus pneumoniae*. Microbiology **144:**3069–3078.
21. **Meinhardt, H., and P. A. de Boer.** 2001. Pattern formation in *Escherichia coli*: a model for the pole-to-pole oscillations of Min proteins and the localization of the division site. Proc. Natl. Acad. Sci. USA **98:**14202–14207.
22. **Meury, J., and G. Devilliers.** 1999. Impairment of cell division in *tolA* mutants of *Escherichia coli* at low and high medium osmolarities. Biol. Cell **91:**67–75.
23. **Pozzi, G., L. Masala, F. Iannelli, R. Manganelli, L. Havarstein, L. Piccoli, D. Simon, and D. A. Morrison.** 1996. Competence for genetic transformation in encapsulated strains of *Streptococcus pneumoniae*: two allelic variants of the peptide pheromone. J. Bacteriol. **178:**6087–6090.
24. **Rothfield, L., S. Justice, and J. Garcia-Lara.** 1999. Bacterial cell division. Annu. Rev. Genet. **33:**423–448.
25. **Thomaides, H. B., M. Freeman, M. El Karoui, and J. Errington.** 2001. Division site selection protein DivIVA of *Bacillus subtilis* has a second distinct function in chromosome segregation during sporulation. Genes Dev. **15:**1662–1673.
26. **Varley, A. W., and G. C. Stewart.** 1992. The *divIVB* region of the *Bacillus subtilis* chromosome encodes homologs of *Escherichia coli* septum placement (*minCD*) and cell shape (*mreBCD*) determinants. J. Bacteriol. **174:**6729–6742.